

Electronic Supplementary Information

Colloidal ZnTe quantum dots-based photocathode with metal-insulator-semiconductor structure towards solar-driven CO₂ reduction to tunable syngas

Peng Wen,^{a‡} Hui Li,^{b‡} Xiao Ma,^b Renbo Lei,^c Xinwei Wang,^c Scott M Geyer^{b*} and
Yejun Qiu^{a*}

^aShenzhen Engineering Lab of Flexible Transparent Conductive Films, School of Materials Science and Engineering, Harbin Institute of Technology, Shenzhen, 518055, P. R. China

^bDepartment of Chemistry, Wake Forest University, Winston-Salem, North Carolina 27109, United States

^cSchool of Advanced Materials, Shenzhen Graduate School, Peking University, Shenzhen 518055, P. R. China

*Corresponding Author

E-mail: yejunqiu@hit.edu.cn E-mail: geyersm@wfu.edu

‡These authors contributed equally to this work.

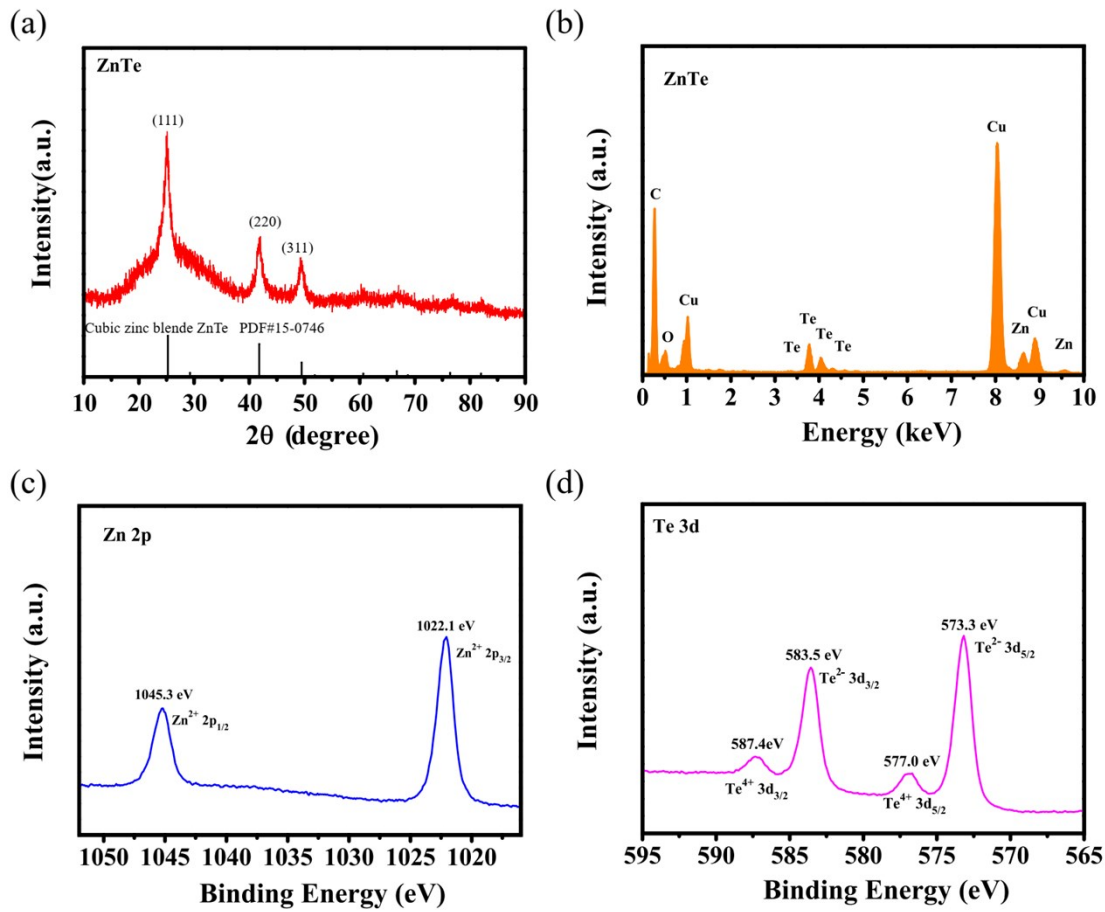


Fig. S1 (a) XRD pattern, (b) EDX spectrum of ZnTe QDs on TEM copper grid, XPS spectra of (c) Zn 2p and (d) Te 3d for the ZnTe QDs.

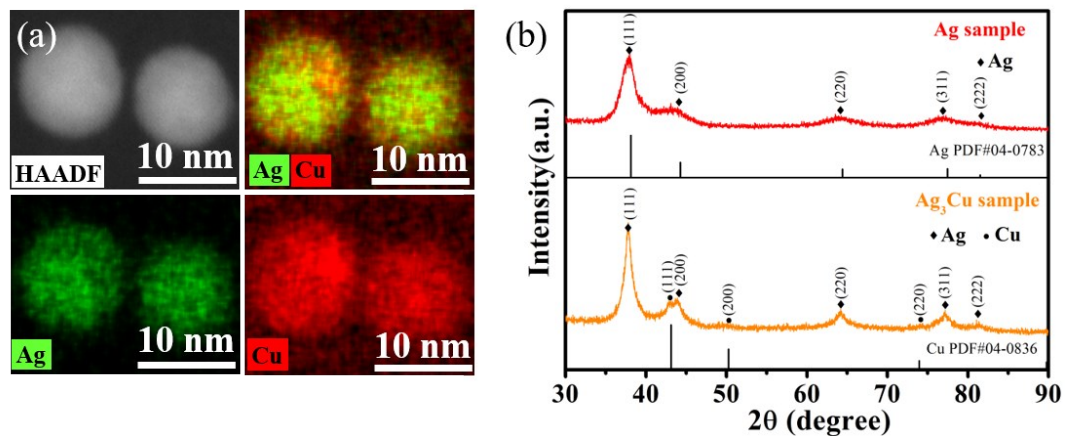


Fig. S2 (a) HAADF-STEM and corresponding EELS mapping of Ag₃Cu NCs, (b) XRD

patterns of Ag_3Cu and Ag NCs.

Table S1

Elemental composition of Ag and Cu in colloidal Ag_3Cu NCs.

Sample	Weight% (ICP-MS)		Atomic ratio (ICP-MS) Ag : Cu
	Ag	Cu	
Ag_3Cu	78.8	15.1	3.07

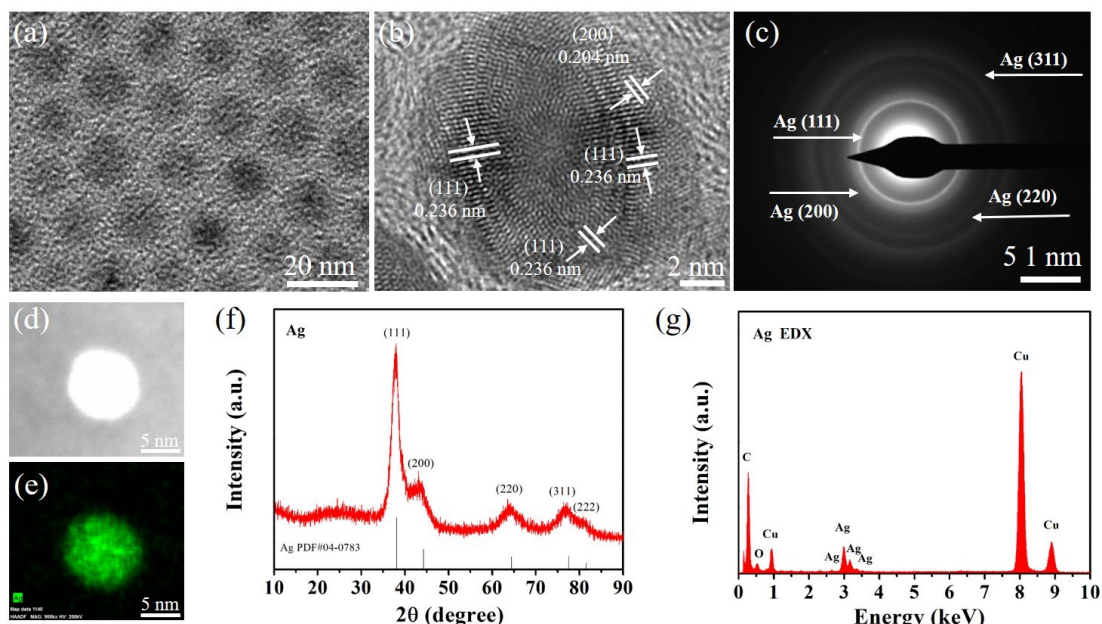


Fig. S3 (a) TEM image, (b) HRTEM image, (c) corresponding SAED pattern, (d) HAADF-STEM, (e) corresponding EELS-elemental mapping image, (f) XRD pattern and (g) EDX spectrum of Ag NCs.

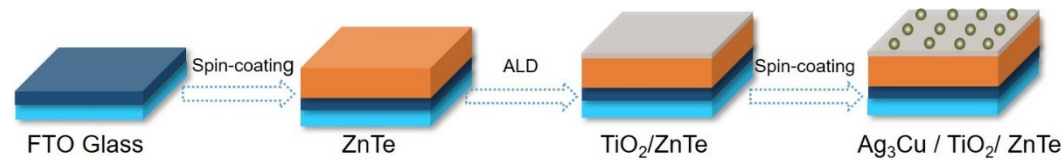


Fig. S4 Schematic of the fabrication procedures of the $\text{Ag}_3\text{Cu}/\text{TiO}_2/\text{ZnTe}$ MIS

photocathode.

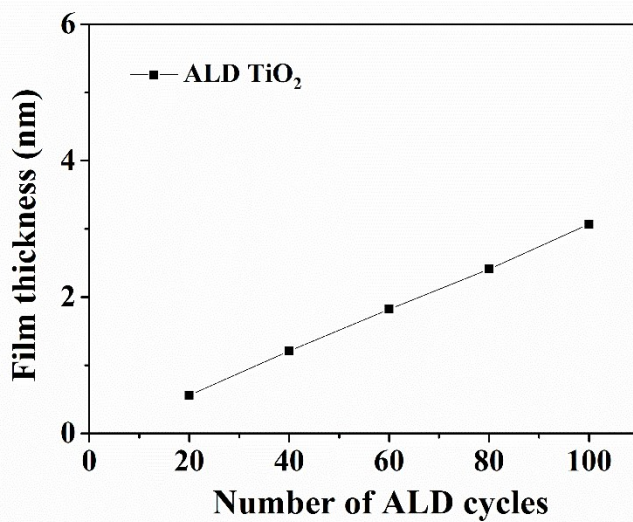


Fig. S5 Thickness of ALD-deposited TiO₂ film determined by ellipsometry results.

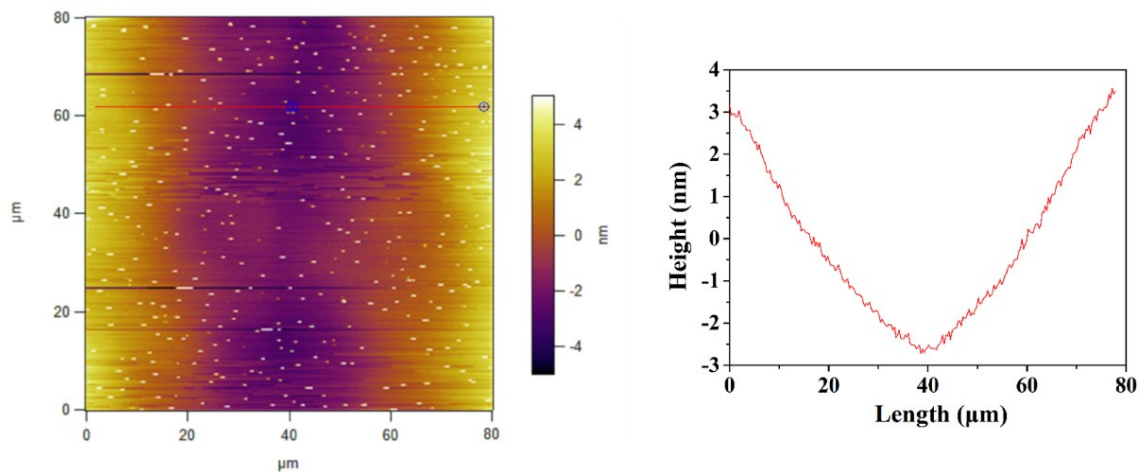


Fig. S6 AFM image of ALD-deposited TiO₂ film on SiO₂/Si substrate.

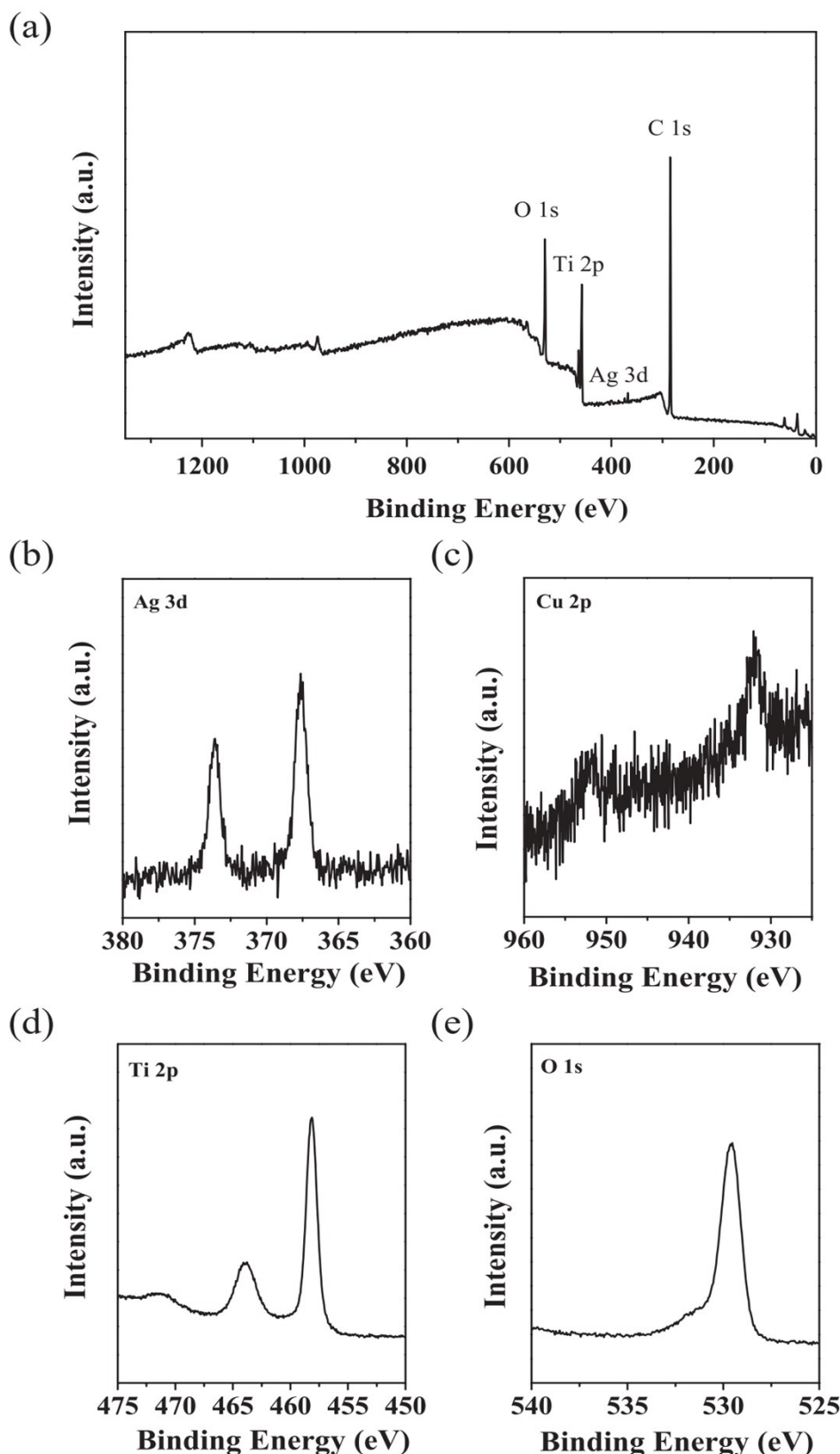


Fig. S7 XPS spectra of $\text{Ag}_3\text{Cu}/\text{TiO}_2/\text{ZnTe}$ sample. (a) XPS survey spectrum and high-resolution XPS spectra of (b) Ag 3d, (c) Cu 2p, (d) Ti 2p and (e) O 1s.

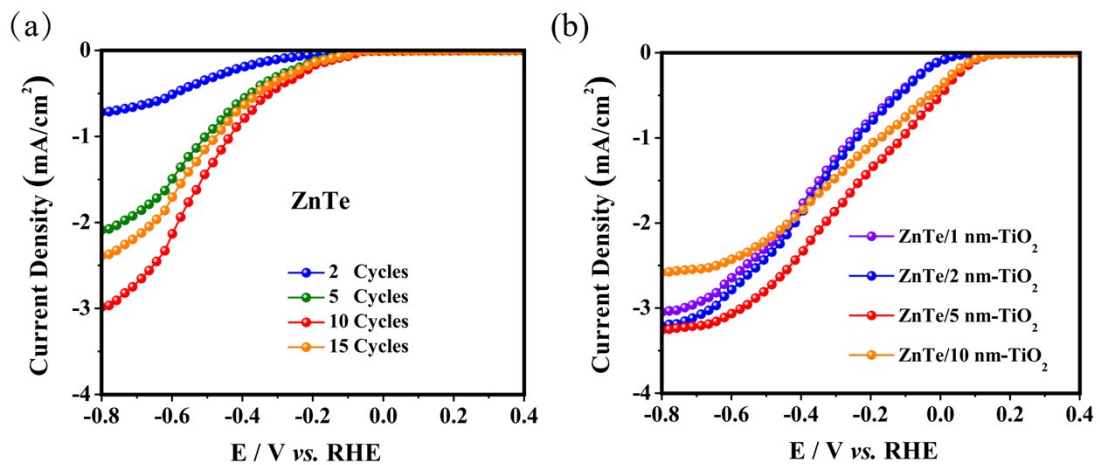


Fig. S8 PEC J - V curves of (a) bare ZnTe photocathodes with different spin-coating cycles and (b) TiO₂/ZnTe-based photocathodes with different covered thickness of TiO₂ in CO₂-saturated 0.1 M KHCO₃ (pH 6.8) under simulated solar irradiation (AM 1.5G, 100 mW/cm²).

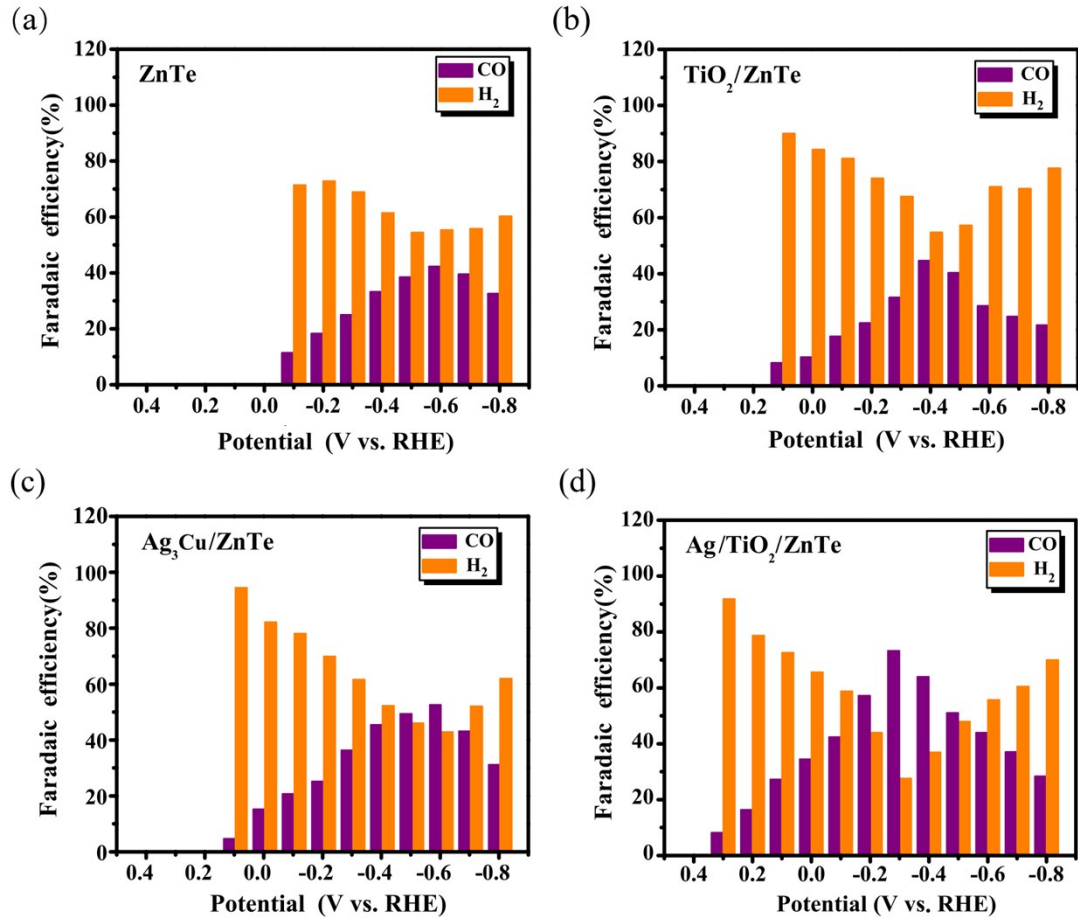


Fig. S9 Faradaic efficiency toward CO and H₂ for (a) ZnTe, (b) TiO₂/ZnTe, (c) Ag₃Cu/ZnTe and (d) Ag/TiO₂/ZnTe photocathodes in CO₂-saturated 0.1 M KHCO₃ electrolyte (pH 6.8) under simulated solar illumination (AM 1.5G, 100 mW/cm²).

Table S2. Comparison of recently reported ZnTe based-photocathodes for PEC CO₂ reduction.

Photocathode	Electrolyte	E_{onset} , (V vs. RHE)	$j_{-0.11 \text{ V}}$ (mA cm ⁻²)	Maximum FE _{CO}	Ref.
ZnO/ZnTe/CdTe/Au	0.5 M KHCO ₃	0.60	-3.88	80%	ACS Nano 2016, 10, 6980–6987
Zn/ZnO/ZnTe	0.5 M KHCO ₃	-0.20	N A	22.9%	Angew. Chem. Int. Ed. 2014, 53, 5852 –5857
ZnO/ZnTe/Au	0.5 M KHCO ₃	-0.10	-3.14	63.0%	Energy Environ. Sci., 2015, 8, 3597--3604
N:C/N:ZnTe	0.5 M KHCO ₃	0.25	-1.21	72.0%	Adv. Energy Mater. 2018, 8, 1702636
PPy/ZnTe	0.1M KHCO ₃	0	N A	13.8%	J. Mater. Chem. A, 2015, 3, 1089–1095
Ag₃Cu/TiO₂/ZnTe	0.1 M KHCO₃	0.40	-3.81	86.5%	This work

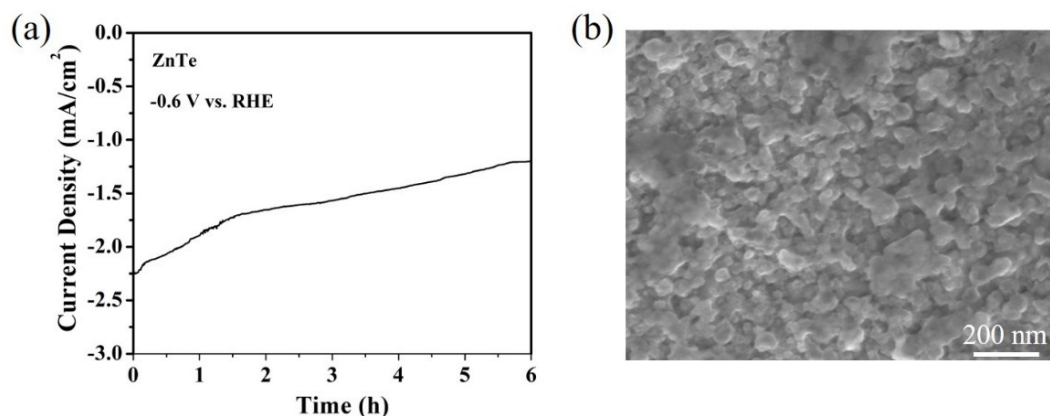


Fig. S10 (a) Time-dependent photocurrents ZnTe photocathode at potential of -0.6 V versus RHE in CO₂-saturated 0.1 M KHCO₃ under simulated solar irradiation and (b) SEM image of ZnTe photocathode after stability measurement.

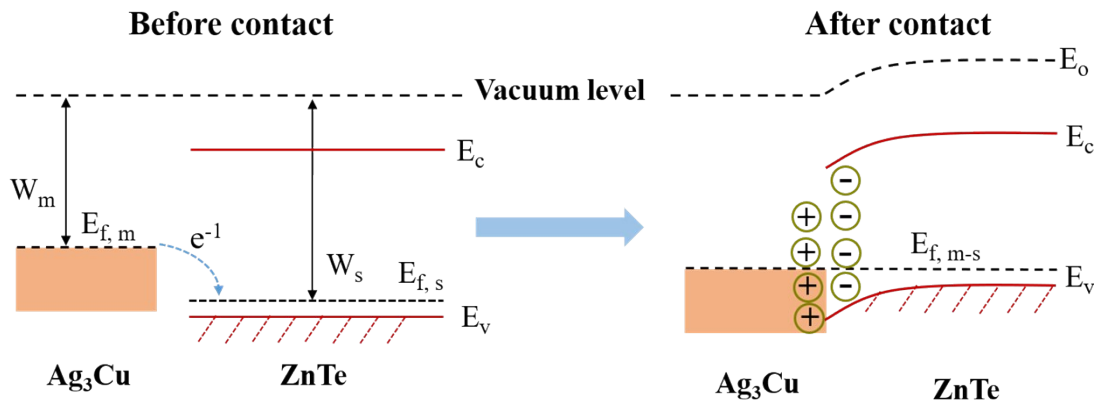


Fig. S11 Schematic diagram of band structure configuration of Ag_3Cu and ZnTe before and after contact.

Table S3

The values of key parameters in Figure 4a, where E_c , E_v , $E_{f,s}$, $E_{f,\text{metal}}$ and E_{reaction} are the conduction band, valance band, Fermi level of ZnTe , Fermi level of metal, and the potential values of the chemical reactions ($E_{\text{H}^+/\text{H}_2}$ and $E_{\text{CO}_2/\text{CO}}$) respectively.

Parameters	$E_{f,\text{Ag}_3\text{Cu}}$	$E_{f,\text{Ag}}$	E_c	E_v	$E_{f,s}$	$E_{\text{H}^+/\text{H}_2}$	$E_{\text{CO}_2/\text{CO}}$
E_{vac} (eV)	-4.37	-4.28	-2.94	-5.23	-4.80	-4.5	-4.39
E_{NHE} (V) pH=0	-0.13	-0.22	-1.56	0.73	0.30	0.00	-0.11

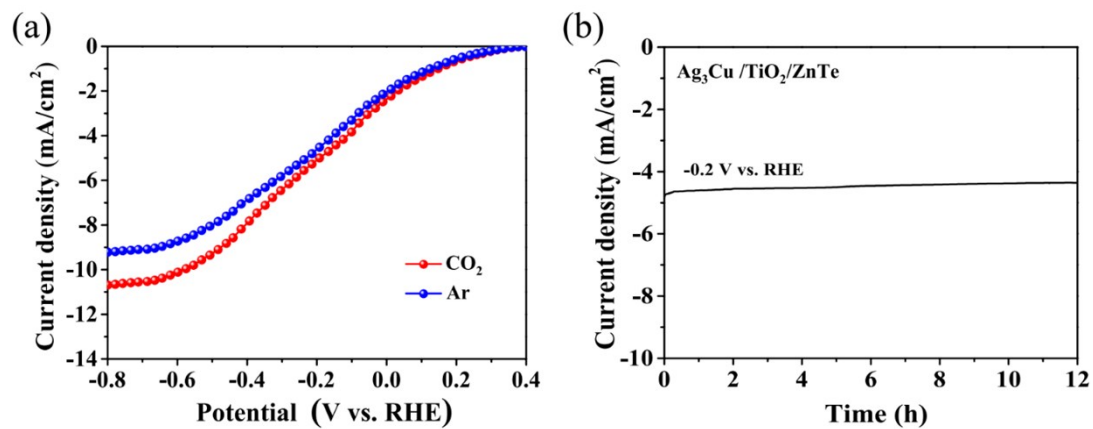


Fig. S12 (a) J-V curves of Ag₃Cu/TiO₂/ZnTe photocathode in CO₂ and Ar-saturated 0.1 M KHCO₃ under simulated solar irradiation, (b) Time-dependent photocurrent of Ag₃Cu/TiO₂/ZnTe photocathode at potential of -0.2 V vs. RHE in Ar-saturated 0.1 M KHCO₃ under simulated solar irradiation.